Facilitation of neural responses to targets moving against optic flow

Sarah Nicholas[a] and Karin Nordström[a,b,1]

[a]Flinders Health and Medical Research Institute, Flinders University, Adelaide, SA 5001, Australia; and [b]Department of Neuroscience, Uppsala University, 751 24 Uppsala, Sweden

Edited by Gwyneth Card, Janelia Research Campus, Ashburn, VA, and accepted by Editorial Board Member Jeremy Nathans July 27, 2021 (received for review December 4, 2020)

For the human observer, it can be difficult to follow the motion of small objects, especially when they move against background clutter. In contrast, insects efficiently do this, as evidenced by their ability to capture prey, pursue conspecifics, or defend territories, even in highly textured surrounds. We here recorded from target selective descending neurons (TSDNs), which likely subserve these impressive behaviors. To simulate the type of optic flow that would be generated by the pursuer's own movements through the world, we used the motion of a perspective corrected sparse dot field. We show that hoverfly TSDN responses to target motion are suppressed when such optic flow moves syn-directional to the target. Indeed, neural responses are strongly suppressed when targets move over either translational sideslip or rotational yaw. More strikingly, we show that TSDNs are facilitated by optic flow moving counterdirectional to the target, if the target moves horizontally. Furthermore, we show that a small, frontal spatial window of optic flow is enough to fully facilitate or suppress TSDN responses to target motion. We argue that such TSDN response facilitation could be beneficial in modulating corrective turns during target pursuit.

target motion | insect vision | sensorimotor | optic flow | TSDN

The survival of many animals may depend on their ability to visually detect small moving objects or targets, as these could represent predators, prey, mates, or territorial intruders (1). Efficient target detection is a computationally challenging task, which becomes even more difficult when done against visual clutter. Despite this, many insects successfully detect targets, followed by highly acrobatic pursuits, often in visually complex environments. For example, male *Eristalis tenax* hoverflies establish territories in foliage rich areas, on alert for intruders or potential mates, and ready to engage in high-speed pursuit (2).

Initial target detection can be facilitated by behaviors that render the background stationary, thus making the target the only thing that moves. Many insects and vertebrates indeed visualize targets against the bright sky (3) or from a stationary stance, such as perching (4–6) or hovering (7, 8). However, as soon as the pursuer moves, its own movement creates self-generated widefield motion across the retina, often referred to as optic flow (9) or background motion (10). In addition to self-generated optic flow, when a pursuer is subjected to involuntary deviations away from their intended flight path, for example by a gust of wind, this also generates optic flow. Quickly correcting such unplanned course deviations is essential for successfully navigating through the world. For example, a flying insect being pushed sideways to the right by a gust of wind, will experience optic flow in the opposite direction. To correct for this, in response to leftward optic flow, the insect will use its wings to perform a corrective optomotor response to the left (11, 12), and/or stabilize its gaze by moving its head (13). Recent evidence suggests that efference copies suppress the visual neurons sensitive to optic flow, as the optomotor response could otherwise counteract voluntary turns (14).

During pursuit, the pursuer is thus subjected to visual motion that could originate from the independent motion of objects within the environment, from its own intentional movements, or from movement imposed by external forces, such as a gust of wind. Importantly, how the insect moves also affects the type of optic flow it will experience. For example, during translations distant features move slower than closer ones, whereas during rotations, all features move at the same angular velocity irrespective of distance from the observer (15). Many insects, including *E. tenax*, seem to use the resulting depth information available in translational motion (2, 16). Moreover, many flying insects, including *Eristalis,* show behavioral segregation between rotational and translational movements (17, 18). How this may influence target detection is currently not known.

The ability of insects to successfully pursue targets in clutter (4, 19) is thus remarkable and suggests a high level of optimization, making the underlying neural mechanisms interesting to study. Indeed, insects that pursue targets, including predatory dragonflies and robberflies, as well as territorial hoverflies, have higher-order neurons in the optic lobes (20, 21) and the descending nerve cord (22, 23) that are sharply tuned to the motion of small, dark targets. Target-tuned neurons often have receptive fields (24–26) in the part of the compound eye that has the best optics (27, 28). Target selective descending neurons (TSDNs) project to the thoracic ganglia (25, 29) where wing and head movements are controlled (30), and electrically stimulating dragonfly TSDNs leads to wing movements (31). Taken together, this suggests that TSDNs subserve target pursuit. However, how TSDNs respond to targets moving against translational and rotational optic flow is unknown.

Significance

Target detection in visual clutter is a difficult computational task that insects, with their poor spatial resolution compound eyes and small brains, do successfully and with extremely short behavioral delays. We here show that the responses of target selective descending neurons are attenuated by background motion in the same direction as target motion but facilitated by background motion in the opposite direction. This finding is important for understanding how target pursuit can occur in tandem with gaze stabilization. Indeed, the neural facilitation would come into effect if the hoverfly is subjected to background motion in one direction but the target it is pursuing moves in the opposite direction and could therefore be used to override gaze stabilizing corrective turns.

Author contributions: S.N. and K.N. designed research; S.N. performed research; S.N. analyzed data; and S.N. and K.N. wrote the paper.

The authors declare no competing interest.

This article is a PNAS Direct Submission. G.C. is a guest editor invited by the Editorial Board.

[1]To whom correspondence may be addressed. Email: karin.nordstrom@flinders.edu.au.

This article contains supporting information online at https://www.pnas.org/lookup/suppl/doi:10.1073/pnas.2024966118/-/DCSupplemental.

Published September 16, 2021.

We quantified the responses of *Eristalis* TSDNs to targets moving against six types of optic flow, three translations and three rotations. The optic flow stimulus was composed of thousands of dots. Thus, the target dot could not be discriminated by shape or contrast but only by its relative motion. We found that optic flow moving syn-directional to the target suppressed the TSDN response, regardless of whether the optic flow moved in a rotational or translational manner. We found that orthogonal optic flow attenuated the TSDN target response but to a lesser degree than syn-directional optic flow. This suggests that the vector divergence between the target and the optic flow is important. Most strikingly, we found that counterdirectional optic flow increased the TSDN response to target motion, if the target moved horizontally. We found that projecting optic flow to only a small frontal portion of the eye was sufficient to elicit both TSDN attenuation and facilitation. As descending neurons control behavioral output (30, 31), the response attenuation and facilitation could play a role in modulating optomotor, or gaze stabilizing corrective turns, as needed during target pursuit.

Results

TSDNs Respond to Target Motion but Not to Optic Flow. We simulated optic flow using the motion of a sparse dot field (24). By projecting the individual features in the sparse dot field onto a screen anterior of the hoverfly, their spatial location, and simulated *z*-depth, over time, provided the type of optic flow that would be generated by self-motion (24). In optic flow–sensitive descending neurons, this stimulus elicits strong direction-selective responses, similar to the responses to widefield sinusoidal gratings (24) or large moving images (22) with naturalistic statistics (32). We recorded from TSDNs (Fig. 1) in male *E. tenax* hoverflies and first confirmed that our optic flow stimulus did not generate a TSDN response (*SI Appendix*, Fig. S1). For example, translational sideslip to the left only generated a response in 18% of 222 repetitions across 12 TSDNs (*SI Appendix*, Fig. S1*A*). Furthermore, when leftward sideslip did generate a TSDN response, this was much less than the response to a target traversing a white background (*SI Appendix*, Fig. S1*B*). This lack of TSDN response confirms that the optic flow stimulus is qualitatively similar to other types of widefield background motion.

In contrast to the lack of response to the optic flow, TSDNs responded strongly to the motion of a small, dark target (22, 24) traversing a white background (compare spiking response during stimulation with the lack of activity before stimulation, Fig. 1 *B*, *Left* and Movies S1 and S2), as well as when the target traversed the stationary sparse dot field (Fig. 1 *B*, *Right* and Movies S3 and S4). Note that since the sparse dot field consisted of hundreds of "targets," there were no spatial characteristics identifying the individual target when both were stationary (Fig. 1 *A*, *Right*). For quantification across neurons, we calculated the mean spike frequency for the duration of target motion, except for the first and last 40 ms of each 500 ms target trajectory (dotted box, Fig. 1 *B* and *C*). We found a small but significant response reduction to targets moving across a stationary dot field compared with a white background (Fig. 1*D*), as expected from the reduced motion energy when the target traversed pattern elements of the stationary dot field. As the response across neurons was variable ($N = 39$, coefficient of variation 62 and 65%, respectively, Fig. 1*D*), we normalized the response from each neuron to its own mean response to a target moving over a white background.

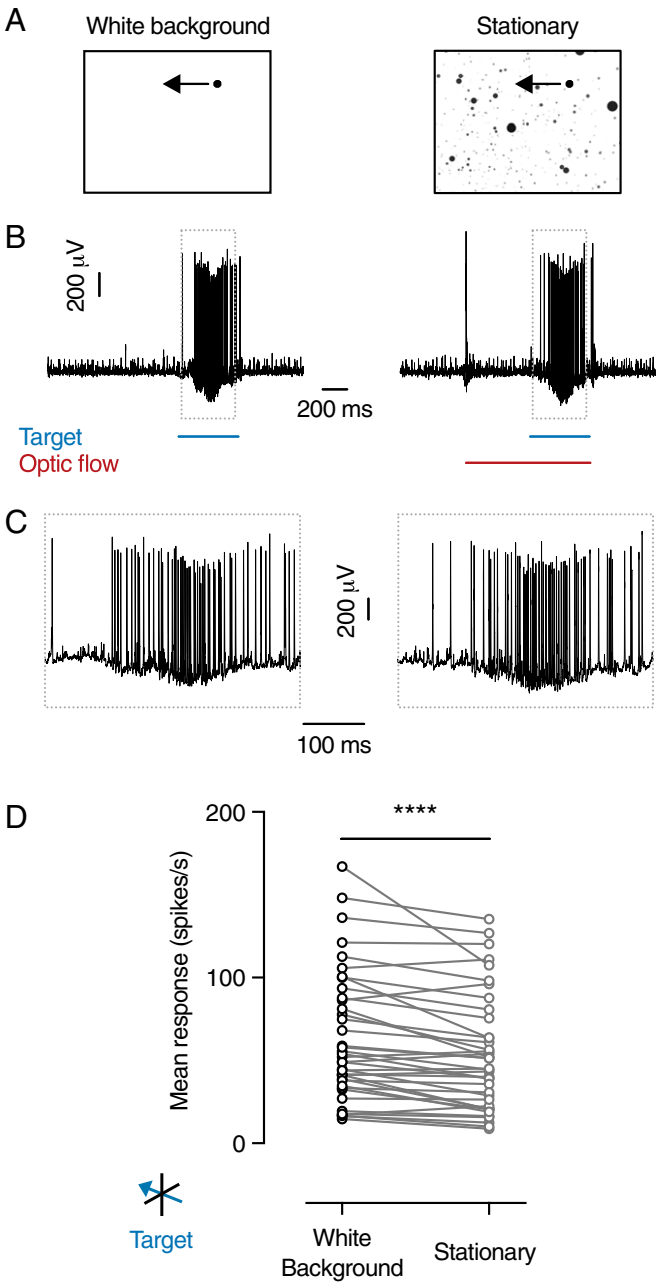

Fig. 1. TSDN response to target motion. (*A*) Pictograms of the round, black target, with a diameter of 3°, traversing a white background (*Left*), or stationary optic flow (*Right*), at 130°/s. (*B*) Raw data trace from an extracellular TSDN recording. Timing of stimulus presentation indicated by colored bars (blue, target, and red, sparse dot field). (*C*) Magnification of the raw data traces shown in *B*. (*D*) The mean spiking response of different TSDNs was significantly reduced when the target moved across a stationary sparse dot field compared with a white background ($N = 39$; $^{****}P < 0.0001$, two-tailed paired *t* test).

Optic Flow Modulates the TSDN Target Response. During translational optic flow, distant features move slower than closer ones, whereas during rotations, all features move at the same angular velocity (15). We asked whether optic flow rotations and translations would therefore have different effects on the TSDN response to target motion. To investigate this, we simulated different types of translations (Fig. 2*A*) at 50 cm/s and rotations (Fig. 2*B*) at 50 deg/s. We found that when the target moved horizontally across syn-directional sideslip, the TSDN response was strongly suppressed (mean inhibition 93%, Fig. 2 *C* and *D*, "Left Sideslip" and Movies S5 and S6), compared with control where the target moved over a stationary dot field (gray, Fig. 2 *C* and *D* and Movies S3 and S4). Similar effects of syn-directional background motion were previously seen when using panoramic images with naturalistic statistics (22). We also found that syn-directional yaw optic flow strongly attenuated the TSDN response to target motion (by

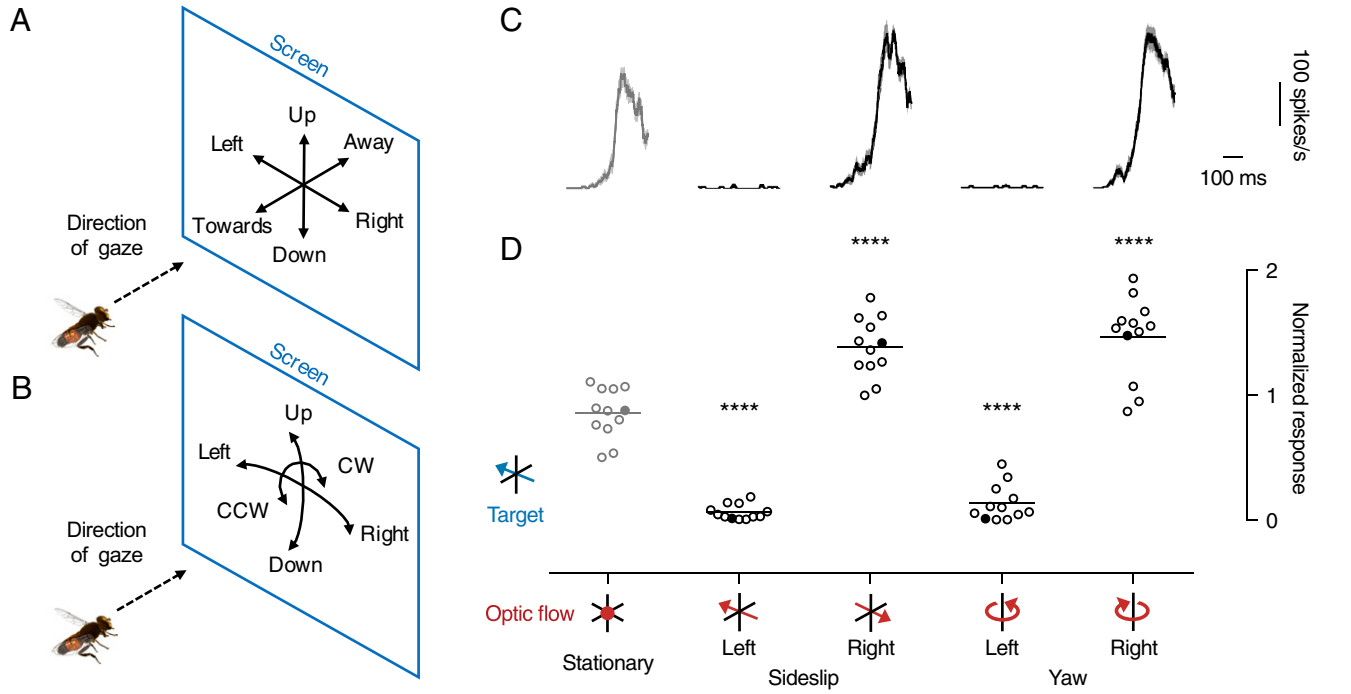

Fig. 2. TSDN response to target motion is affected by horizontal optic flow. (*A*) Pictogram indicating the three different types of translations, as seen by the hoverfly. Sideslip was displayed to the left or the right, lift up or down, and thrust toward or away from the hoverfly, all at 50 cm/s. (*B*) The three different types of rotations used. As these were simulated to rotate around the hoverfly's position (24), the optic flow displayed on the screen can be described as yaw to the left or the right, pitch up or down, and clockwise or counterclockwise roll, all at 50 deg/s. (*C*) The TSDN response to a target traversing a stationary sparse dot field (*Left*, gray), sideslip or yaw, either syn-directional or counterdirectional to the target (red pictograms). All histograms from a single TSDN (mean ± SEM, $n = 18$) shown with 1-ms resolution after smoothing with a 20-ms square-wave filter. (*D*) The mean response across TSDNs ($N = 12$) to a target traversing stationary optic flow (*Left*, gray), sideslip or yaw, syn-directional ("*Left*") or counterdirectional ("*Right*") to the target, after normalizing the data to each neuron's own response to a target traversing a white background. The lines show the mean, and the filled data points correspond to the neuron in *C*. In *D*, significance is shown with **** for $P < 0.0001$ using a one-way ANOVA followed by Dunnett's multiple comparison's test done together with the data shown in Fig. 4*B*.

84%, Fig. 2 *C* and *D*, "Left Yaw"). This suggests that rotational and translational optic flow have the same effect on TSDN responses to target motion, thereby rejecting the hypothesis that the relative motion of features within the optic flow is important.

We next asked whether counterdirectional optic flow would also attenuate the TSDN response to target motion but less than syn-directional optic flow. However, we found that when the target moved over counterdirectional sideslip the TSDN response was strongly enhanced (mean increase 71%, Fig. 2 *C* and *D*, "Right Sideslip" and Movies S7 and S8). Similarly, yaw moving counterdirectional to the target also facilitated the TSDN response, by 85% (Fig. 2 *C* and *D*, "Right Yaw"). Such response facilitation was not seen when displaying targets over counterdirectional background motion using panoramic images, in either TSDNs (22) or other target-tuned neurons in the fly optic lobes (21, 26, 33). This rejects the hypothesis that counterdirectional optic flow attenuates TSDNs.

Frontal Optic Flow Is Required and Sufficient. Our data show that yaw and sideslip have similar effects on TSDN responses to target motion (Fig. 2 *C* and *D*). As both sideslip and yaw contain substantial local motion in the frontal visual field (34), we next asked if frontal optic flow is required. We investigated this by limiting the spatial extent of the sideslip to either cover the ipsilateral, dorsal, ventral, or contralateral position on the screen (Fig. 3*A*). Note that only the dorsal position covers the TSDN receptive field (Fig. 3*A*). In the other three positions, the sideslip optic flow was spatially separated from the receptive field (Fig. 3*A*) and thus the target trajectory.

We found that when sideslip moved syn-directional to the target, the TSDN response was attenuated if the optic flow covered the full, dorsal, or ventral position on the screen (Fig. 3*B*), compared with the stationary control (gray, Fig. 3*B*). However, when the optic flow only covered the ipsilateral or contralateral positions, there was no difference compared with control (Fig. 3*B*), suggesting that frontal optic flow is both required and sufficient. Previous work using moving images with naturalistic statistics showed that these did not have to spatially overlap with the target trajectory, nor have a large spatial extent, to attenuate TSDN responses (22).

We next found that when sideslip moved counterdirectional to the target, the TSDN response to target motion was facilitated if the optic flow covered the full, dorsal, or ventral positions of the screen (Fig. 3*C*). When the sideslip was limited to the ipsilateral or contralateral positions, there was no TSDN response facilitation (Fig. 3*C*). This suggests that the optic flow does not have to spatially overlap with the target trajectory. However, there has to be frontal, counterdirectional optic flow for facilitation to take place.

In summary, our results show that a small spatial window of optic flow in either the dorsal or ventral visual field is enough to strongly attenuate (Fig. 3*B*) or facilitate (Fig. 3*C*) the TSDN response to target motion.

Vector Divergence between Target and Optic Flow Affects TSDNs Response. Our data above (Figs. 2 and 3) show that syn-directional optic flow strongly attenuates TSDN responses to target motion, whereas counterdirectional optic flow facilitates the response. This suggests that the level of vector divergence between the target and the optic flow influences the TSDN responses, so that maximum

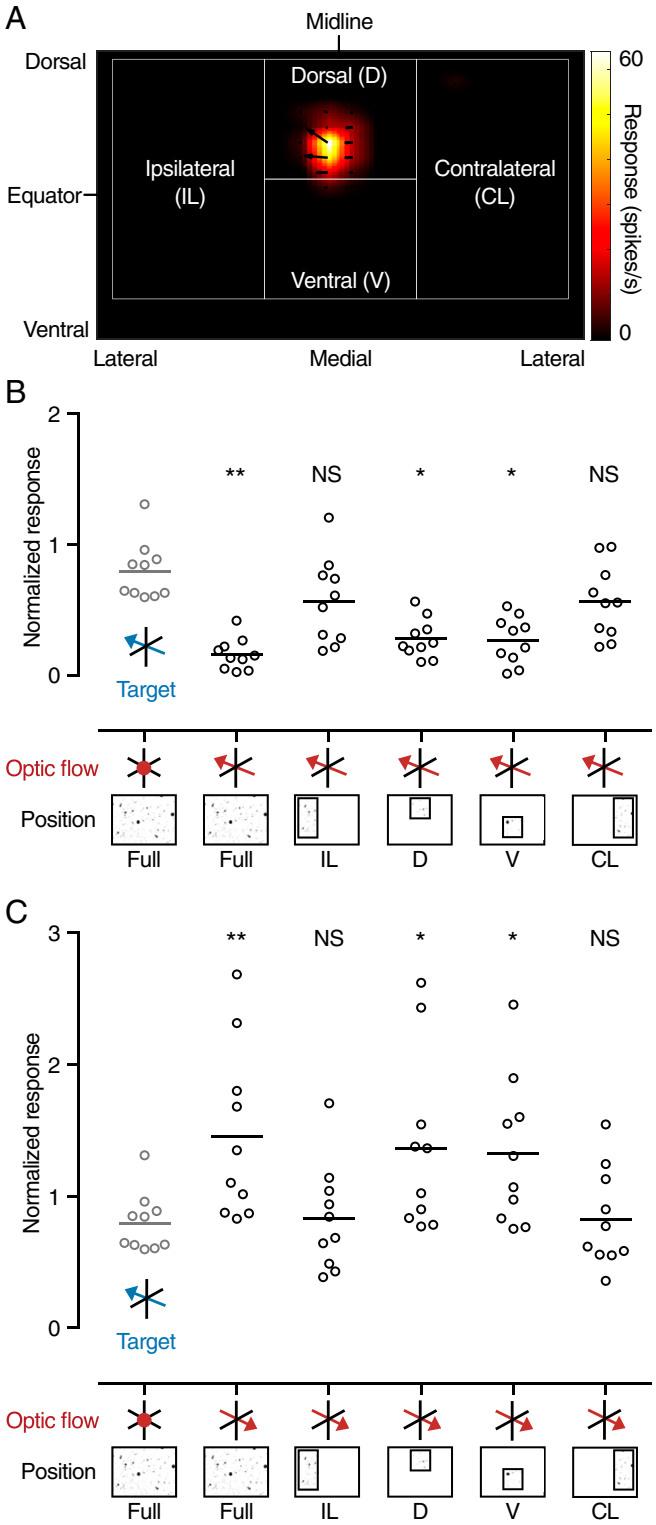

Fig. 3. Frontal optic flow is required and sufficient. (*A*) Pictogram of the separation of the optic flow into four distinct positions: ipsilateral (IL), dorsal (D), ventral (V), and contralateral (CL). The color coding shows the receptive field of an example TSDN and the arrows its local motion sensitivity. (*B*) TSDN responses to targets moving over syn-directional sideslip are significantly attenuated compared to stationary control (gray) if the sideslip covers the full, dorsal, or ventral screen. (*C*) TSDN responses to targets moving over counterdirectional sideslip are significantly facilitated compared to stationary control (gray, same data as in *B*) if the sideslip covers the full, dorsal, or ventral visual field. *B* and *C* show data from the same neurons ($N = 10$, one-way ANOVA followed by Dunnett's multiple comparisons test, with $^*P < 0.05$, $^{**}P < 0.01$ and NS for $P > 0.05$). The lines show the mean.

attenuation is generated at minimum vector divergence, whereas maximum facilitation is generated at maximum divergence. To explore this, we quantified the effect other types of optic flow had on TSDN responses to target motion.

We found that the TSDN target response was suppressed by lift, which moves orthogonal to the target (mean 44% suppression for downward lift, "Lift Down;" 34% for upwards lift, "Lift Up," Fig. 4). When the target was displayed against pitch, which also provides orthogonal motion in the frontal visual field, the response was also suppressed (mean 57% suppression, "Pitch Down;" 55% for "Pitch Up," Fig. 4). The TSDN response to target motion was also attenuated when the target was displayed against thrust, which provides orthogonal motion along the animal's anterior–posterior axis (mean 44% suppression for "Thrust Towards;" 58% for "Thrust Away," Fig. 4). Thus, orthogonal optic flow attenuates the TSDN response (Fig. 4) but not as much as syn-directional optic flow (Fig. 2).

We next looked at roll optic flow, which creates no local motion straight ahead of the fly but opposite direction local motion in the dorsal and ventral visual fields. For example, during counterclockwise roll ("Roll CCW," Fig. 4) the target and the optic flow move in the same direction through the dorsal receptive field but in opposite directions in the ventral visual field. Therefore, the TSDN would receive a combination of maximum and minimum vector divergence signals from the "dorsal" and "ventral" parts (as shown in Fig. 3*A*). We found that the response attenuation was stronger against counterclockwise roll (mean suppression 75% for "Roll CCW," Fig. 4) than against clockwise roll (32%, "Roll CW," Fig. 4).

Thus, our data (Figs. 2 and 4) support the notion that the level of vector divergence influences the TSDN response. To explore this in further detail, we recorded from TSDNs that respond robustly both to horizontal (gray, Fig. 5 *A* and *B*) and vertical target motion (black, Fig. 5 *A* and *B*). We found that when the target moved horizontally, the TSDN response was strongly attenuated against syn-directional sideslip (second column, Fig. 5*C*), strongly facilitated when displayed against counterdirectional sideslip (third column, Fig. 5*C*), and less attenuated against orthogonal lift in either direction (last two columns, Fig. 5*C*), consistent with previous results (Figs. 2 and 4). In the same eight TSDN neurons, we next moved the target vertically. We found that the TSDN response was completely attenuated against syn-directional lift (last column, Fig. 5*D*) and less attenuated against orthogonal sideslip in either direction (second and third column, Fig. 5*D*). This supports the suggestion that maximum TSDN response attenuation is generated at minimum vector divergence between the target and optic flow. However, when the vertical target was displayed against counterdirectional lift (fourth column, Fig. 5*D*), there was no response facilitation. This suggests that maximum vector divergence on its own is not enough to explain the TSDN response facilitation to target motion.

Optic Flow at Different Dot Densities Modulates TSDN Responses. The experiments above (Figs. 1–5) used optic flow with dot densities of 100 per m^3. Is it possible that the optic flow's effect on TSDN responses depends on the dot density? To investigate this, we used six different dot densities, ranging from 10/m^3 to 500/m^3 (*SI Appendix*, Fig. S2 *A* and *B*). All dot densities had naturalistic Fourier spectra (*SI Appendix*, Fig. S2*C*), and the contrasts ranged from below naturalistic (35) for the sparsest, to above naturalistic for the densest (*SI Appendix*, Fig. S2*D*). We verified that optic flow with these dot densities stimulated optic flow–sensitive descending neurons (*SI Appendix*, Fig. S2*E*).

We first quantified the TSDN response to a target moving over stationary optic flow and found that this remained robust across dot densities (gray data, Fig. 6). We next quantified the TSDN response to targets moving over syn-directional sideslip and found that this was significantly inhibited compared with stationary

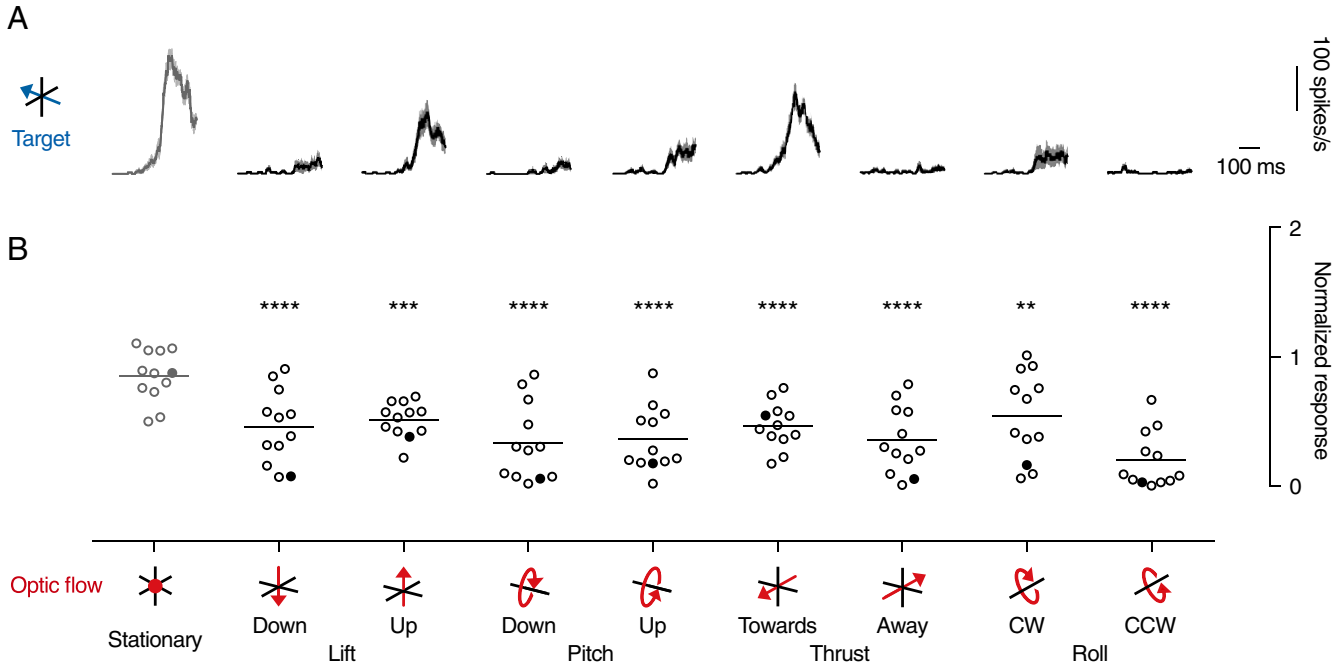

Fig. 4. The TSDN response to target motion is attenuated by orthogonal optic flow. (*A*) The response from one TSDN to a target traversing a stationary sparse dot field (*Left*, gray, replotted from Fig. 2*C*) or different types of optic flow (red pictograms). All histograms shown as mean ± SEM ($n = 18$) at 1-ms resolution, after smoothing with a 20-ms square-wave filter. (*B*) The mean response across TSDNs ($N = 12$, same neurons as Fig. 2*D*) to a target traversing a stationary sparse dot field (*Left*, gray, replotted from Fig. 2*D*) or different types of optic flow. Stars indicate significance, one-way ANOVA followed by Dunnett's multiple comparisons test (**$P < 0.01$, ***$P < 0.001$, and ****$P < 0.0001$), done together with the data shown in Fig. 2*D*. Translations were simulated at 50 cm/s and rotations at 50°/s. The lines show the mean, and the filled data points correspond to the neuron in *A*.

control at all dot densities (two-way ANOVA, $P < 0.0001$, Fig. 6). In contrast, when the target moved over counterdirectional sideslip, there was no facilitation at the lowest dot density (Fig. 6*A*). However, the facilitation was significant for dot densities of 50/m^3 to 500/m^3 (two-way ANOVA, $P < 0.0001$, Fig. 6 *B*–*F*). Our data thus suggest that the effect optic flow has on TSDN target responses does not depend on dot density, at least not for the densities tested here (two-way ANOVA, $P = 0.2399$, Fig. 6).

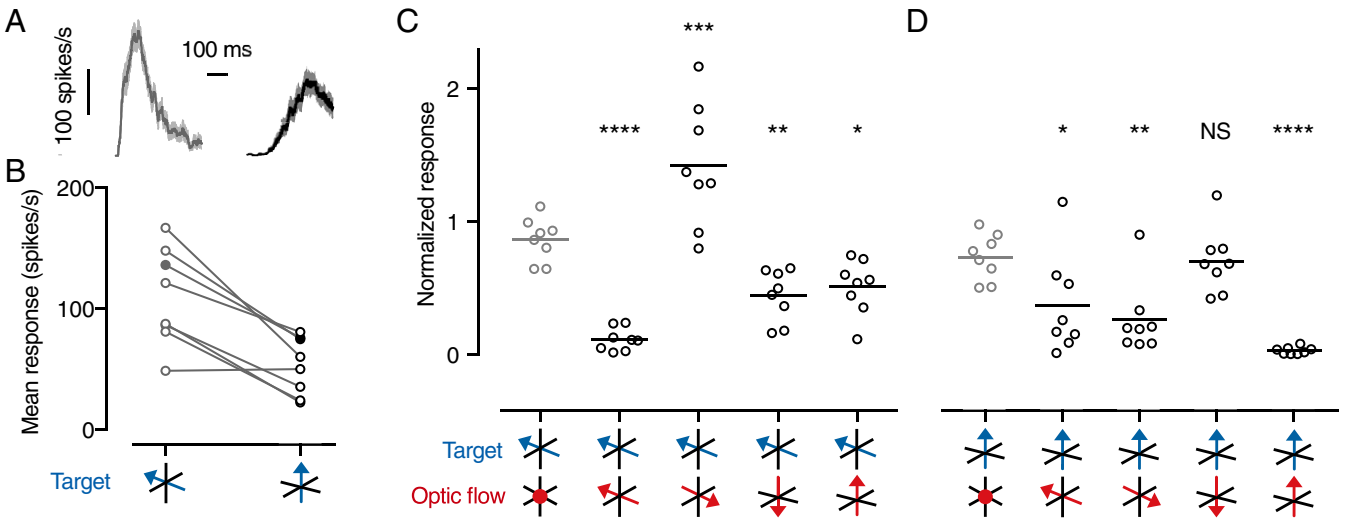

Fig. 5. Vector divergence between optic flow and target. (*A*) The TSDN response to a target traversing a white background horizontally (*Left*, gray) or vertically (*Right*, black). Histograms shown as mean ± SEM ($n = 18$) at 1-ms resolution, after smoothing with a 20-ms square-wave filter. (*B*) The mean spiking response of eight TSDNs to targets moving horizontally (gray, *Left*) or vertically (black, *Right*) over a white background. The filled data points correspond to the neuron in *A*. (*C*) TSDN responses to targets moving horizontally across sideslip or lift, syn-directional, counterdirectional, or orthogonal to the target, as indicated by the pictograms. Significance shown using one-way ANOVA followed by Dunnett's multiple comparisons test, with *$P = 0.0232$, **$P = 0.006$, ***$P = 0.0003$, and ****$P < 0.0001$. (*D*) TSDN responses to targets moving vertically across sideslip or lift, orthogonal, counterdirectional, or syn-directional to the target, as indicated by the pictograms. Significance shown using one-way ANOVA followed by Dunnett's multiple comparisons test, with *$P = 0.0198$, **$P = 0.0021$, ****$P < 0.0001$, and NS for $P > 0.05$. Same $N = 8$ in *B*–*D*.

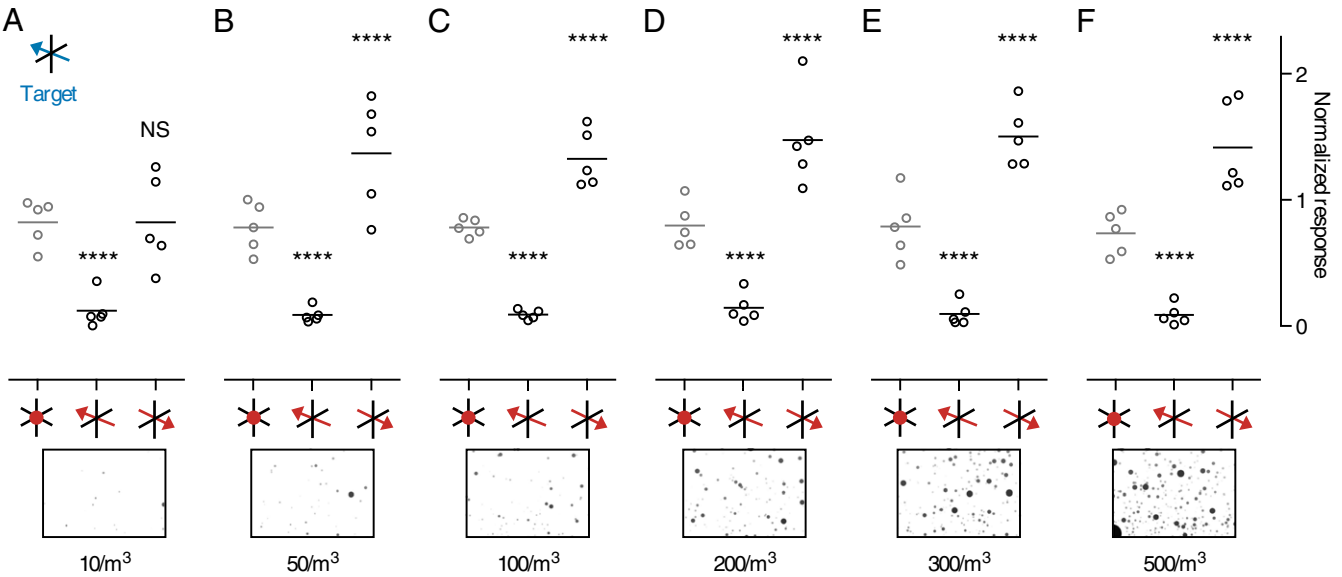

Fig. 6. The density of the optic flow has no strong effect on TSDN responses. (*A*) TSDN responses to a target moving over optic flow with a density of 10 dots/m^3. (*B*) TSDN responses to a target moving over optic flow with a density of 50 dots/m^3. (*C*) Responses to a target moving over optic flow with a density of 100 dots/m^3. (*D*) Responses when the optic flow had a density of 200 dots/m^3. (*E*) Responses when the optic flow had a density of 300 dots/m^3. (*F*) Responses when the optic flow had a density of 500 dots/m^3. In all panels, the gray data points show the responses to a target moving over a stationary dot field, followed by syn-directional and counterdirectional sideslip. Significance shown using two-way ANOVA followed by Dunnett's multiple comparisons test, with ****$P <$ 0.0001 and NS for $P > 0.05$. Same $N = 5$ in all panels.

Our data suggest that there are differences between the TSDN response suppression and facilitation (Figs. 5 and 6). To determine whether there are other differences, we investigated if the inhibition or facilitation was affected by preceding optic flow (green, *SI Appendix*, Fig. S3*A*). During target motion (blue, *SI Appendix*, Fig. S3*A*), the concurrent optic flow (red, *SI Appendix*, Fig. S3*A*) was either stationary or moving. We found that preceding optic flow affected the TSDN response if it was syn-directional (*SI Appendix*, Fig. S3*B*) but that counterdirectional preceding optic flow did not (*SI Appendix*, Fig. S3 *D* and *E*). This supports the suggestion that there are different circuit mechanisms driving TSDN response suppression and facilitation.

Responses to ON–OFF Edges Consistent with 1-Point Correlation. TSDNs have been proposed to get their input from small target motion detectors (STMDs, see ref. 36). As opposed to our TSDN data, hoverfly STMD responses are rarely suppressed by syn-directional background motion and not facilitated by counter-directional background motion (21). As there are many other target-tuned neurons in the fly optic lobes (e.g., refs. 33 and 37–40), it is possible that TSDNs do not get their input from STMDs. We can investigate the potential input using the underlying target tuning mechanisms, which can be distilled down into three fundamentally different concepts. For example, visual neurons can become target tuned by receiving inhibitory feedback from the widefield system (40–42) or by using center-surround antagonism together with rapid adaptation (39, 43). Alternatively, they can use an elementary STMD model, which is tuned to the unique spatiotemporal profile of a moving target, with a dark-contrast change (OFF) from the leading edge followed by a bright-contrast change (ON) by the trailing edge. Importantly, while the first two mechanisms rely on comparisons from neighboring points in space, the elementary STMD compares input from one point in space (39, 44, 45). Therefore, the first two models will respond similarly to the motion of a target, to the motion of a leading OFF edge, and the motion of a trailing ON edge (black, Fig. 6, redrawn from refs. 39 and 46). In contrast, the elementary STMD model only responds strongly to the target (gray, Fig. 7, redrawn from ref. 46).

Our results show that TSDNs do not respond well to a leading OFF edge or to a trailing ON edge (white, Fig. 7). However, a complete target, where the leading edge is rapidly followed by a trailing edge, gives a robust TSDN response (white, Fig. 7). Indeed, the physiological responses (white, Fig. 7) match the elementary STMD model output (gray, Fig. 7). Since STMD physiology also matches the elementary STMD model output (46, 47), this suggests that TSDNs receive input from STMDs.

Discussion

We found that optic flow moving syn-directional to a target almost completely attenuated the TSDN target response (Fig. 2), even when the optic flow only covered a small part of the frontal visual field (Fig. 3). More strikingly, we found that optic flow counter-directional to target motion increased the TSDN response (Fig. 2), if the target moved horizontally (Fig. 5), across a range of dot densities (Fig. 6). We also found that orthogonal optic flow attenuated the TSDN target response (Figs. 4 and 5), but less than syn-directional motion, suggesting that the vector divergence between the target and the optic flow is important for response suppression. However, we found that vector divergence was not enough to explain the response facilitation (Fig. 5*D*).

We show that TSDN responses to target motion are facilitated by counterdirectional optic flow (Fig. 2). Such neural facilitation has not been seen in previous work in TSDNs (22), STMDs (21, 26, 47), or other target-tuned neurons in the optic lobes (33, 37, 40). Instead, in our previous work TSDN responses were significantly reduced when a background image with naturalistic statistics moved counterdirectional to the target (22). Since the backgrounds used previously drive optic flow–sensitive descending neurons as well as sinusoidal gratings do (22, 48), and as well as the sparse dot field used here (*SI Appendix*, Fig. S2*E* and ref. 24), this suggests that TSDN response facilitation is not generated by widefield motion in general. Instead, this suggests that there is something fundamentally different about the optic flow used here and the backgrounds in previous work. One difference is that we

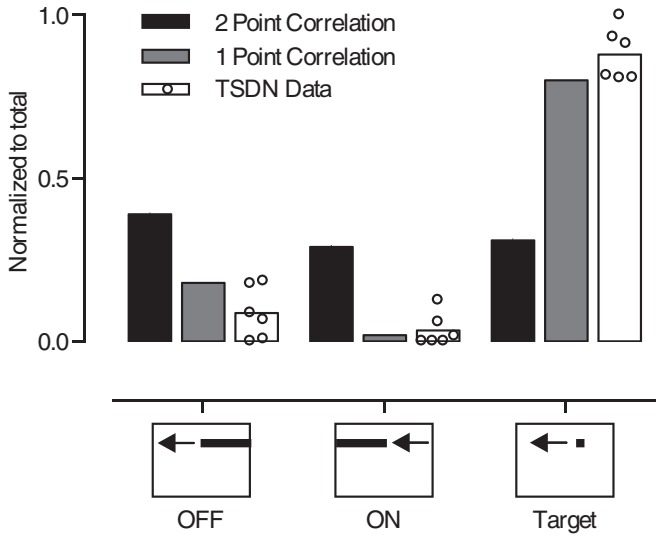

Fig. 7. Elementary STMD input to TSDNs. Responses to a leading OFF edge, trailing ON edge, or a complete black target, with a side of 3°, traversing a white background at 130°/s. The black data show the predicted output from a motion detector that compares luminance changes from at least two points in space. Data replotted from ref. 46, after normalizing to its own sum. The gray data show the predicted output from an elementary STMD, which compares luminance changes from one point in space. Data replotted from ref. 46, after normalizing to its own sum. The white data show the TSDN response to the same three stimuli ($N = 6$) after normalizing the data from each neuron to its own sum.

here use perspective corrected optic flow, where the individual features move faster the closer they are during translations, whereas during rotations they all move at the same angular velocity irrespective of distance from the viewer. However, we found that the facilitation was strong whether the target moved over sideslip or yaw (Fig. 2), suggesting that the relative motion of the features within the optic flow is not important.

Another difference is that the optic flow used here consisted of the motion of thousands of "targets," whereas previous TSDN work used background images (22). Our data show that there was no facilitation if the dot density decreased too much (Fig. 6*A*), suggesting that the number of features moving through the frontal visual field might be important. In addition, it is currently unknown how STMDs, which are likely presynaptic to the TSDNs (Fig. 7, and see ref. 36), respond to sparse dot fields. However, we do know that STMDs generate their ability to detect targets in clutter by being sharply tuned to the target's unique spatiotemporal profile (44), with a dark-contrast OFF edge quickly followed by a bright-contrast ON edge (Fig. 7). Indeed, if naturalistic backgrounds contain small, high-contrast features, these often generate STMD responses (47). However, despite our optic flow consisting of "targets," we saw no consistent TSDN responses even to preferred direction motion (e.g., "Sideslip Left," "Yaw Left," *SI Appendix*, Fig. S1 and Movies S5 and S6). This suggests that TSDNs do not filter contrasting targets embedded within a background, like some STMDs do (21, 47).

It is thus difficult to determine whether the facilitation is driven by active facilitation onto the TSDN or if it is inherited from upstream processes. Since the optic flow did not have to spatially overlap with the TSDN receptive field or the target trajectory (Fig. 3 *A* and *C*), the facilitation is unlikely to be generated by feedback of the TSDN onto itself, for example. Since the facilitation required frontal optic flow, it could come from a direction-selective neuron type with a frontal visual field. Since counter-directional lift did not facilitate the TSDN response if the target moved vertically rather than horizontally (Fig. 5*D*), such a neuron might have to be more sensitive to horizontal motion than to vertical motion. Since some STMDs might respond to features within the optic flow used here (47), and furthermore, since there are some STMDs that respond both to target motion and to features within background motion (21), these could potentially play a role in facilitation. Future investigation of STMD and TSDN responses are clearly required to explore the underlying mechanisms.

We found some notable differences between attenuation and facilitation. For example, as opposed to the response attenuation, there was not facilitation to the lowest dot density (Fig. 6*A*), and whereas attenuation was affected by preceding optic flow (*SI Appendix*, Fig. S3*B*), facilitation was not (*SI Appendix*, Fig. S3 *D* and *E*). In addition, only horizontally moving targets could be facilitated (Fig. 5*D*). Taken together, this suggests that the underlying circuit mechanisms differ. The response suppression could be driven by active inhibition from widefield motion detectors, as previously suggested (22), or inherited from upstream processes. We previously showed that TSDN responses to target motion are suppressed by background motion consisting of an image with naturalistic statistics and that background stimuli that drive optic flow–sensitive neurons suppress TSDN responses to target motion, whether spatially overlapping with the target trajectory or not (22). Indeed, we here confirmed that stimuli that drive optic flow–sensitive neurons (*SI Appendix*, Fig. S2*E*) suppress TSDN responses to target motion (Fig. 6), whether overlapping or not (Fig. 3*B*). Thus, TSDNs appear to be suppressed by widefield motion in general.

Nevertheless, our findings make behavioral sense (*SI Appendix*, Fig. S4). Prior to initiating target pursuit, male *Eristalis* hoverflies predict the flight course required to successfully intercept the target, based predominantly on the target's angular velocity (49). To successfully execute an interception flight, the hoverfly turns in the direction that the target is moving (49). In doing so, the hoverfly creates self-generated optic flow counterdirectional to the target's motion. In this case, the TSDNs would be facilitated (Fig. 2), which could be beneficial. Importantly, the facilitation would take place across a range of dot densities (Fig. 6 *B–F*), suggesting that even relatively sparse background textures (*SI Appendix*, Fig. S2*B*) would affect the TSDN response.

Once pursuit is initiated, if the pursuer drifts rightward due to, for example, a gust of wind, this induces leftward optic flow across the frontal retina, which would evoke a leftward optomotor response and/or gaze stabilizing turn (red, *SI Appendix*, Fig. S4 *B*, *Left*). If the target was also moving leftward, in the direction of the corrective maneuver, this maneuver would also pursue the target, and no TSDN signal would be required (*SI Appendix*, Fig. S4 *C*, *Left*). Indeed, we found that the TSDNs were quiet under such conditions ("*Left*," Fig. 2). However, if the optic flow instead moved rightward, counterdirectional to the target, the TSDNs would be strongly facilitated ("*Right*," Fig. 2 and *SI Appendix*, Fig. S4 *C*, *Right*). Considering that TSDNs project to motor command centers in the thoracic ganglia (25, 31), such TSDN facilitation could then potentially override corrective turns. The TSDN response modulation by optic flow shown here could thus be beneficial for controlling behavioral output.

We only saw response facilitation if the target moved horizontally and not vertically (Fig. 5). This facilitation difference could be affected by the fact that the TSDNs that we recorded from responded better to horizontal motion than to vertical target motion (Fig. 5 *A* and *B*). In addition, it is currently unknown whether hoverfly TSDNs control head movements, wing movements, or maybe both. Indeed, recent work suggests that gaze stabilizing turns by the head, and the wing optomotor response, are controlled independently and by different visual components (13, 50, 51). Furthermore, the difference could be explained by different behavioral strategies used for vertical and horizontal target deviations (52). For example, whereas horizontal deviations

require the left and right wings to move differently, to induce a directional turn, vertical deviations would likely require the left and right wings to move similarly. Finally, it is important to note that even if the responses to vertical target motion were not facilitated, neither were they suppressed (fourth column, Fig. 5*D*). There would thus still be a strong neural signal projected to the thoracic ganglia.

Materials and Methods

Electrophysiology. *E. tenax* hoverflies were reared and maintained as previously described (53). For electrophysiology, a male hoverfly was immobilized ventral side up using a beeswax and resin mixture. A small hole was cut at the anterior end of the thorax to expose the cervical connective, which was then raised slightly and supported using a small wire hook, for insertion of a sharp polyimide-insulated tungsten microelectrode (2 MOhm, Microprobes). The animal was grounded via a silver wire inserted into the ventral part of the hole.

Extracellular signals were amplified at 100× gain and filtered through a 10- to 3,000-Hz bandwidth filter on a DAM50 differential amplifier (World Precision Instruments), with 50 Hz noise removed with a HumBug (Quest Scientific). The data were digitized via Powerlab 4/30 (ADInstruments) and acquired at 40 kHz with LabChart 7 Pro software (ADInstruments). Single units were discriminated by amplitude and half-width using Spike Histogram software (ADInstruments).

Visual Stimuli. *Eristalis* males were placed ventral side up, centered and perpendicular to an Asus liquid-crystal display (LCD) at 6.5 cm distance. The screen had a refresh rate of 165 Hz, a linearized contrast with a mean illuminance of 200 Lux, and a spatial resolution of 2,560 × 1,440 pixels, giving a projected screen size of 155° × 138°. Visual stimuli were displayed using custom written software based on the Psychophysics toolbox (54, 55) in Matlab (Mathworks).

TSDNs were identified as described (22, 24). In short, we mapped the receptive field of each neuron by scanning a target horizontally and vertically at 20 evenly spaced elevations and azimuths (24) to calculate the local motion sensitivity and local preferred direction. We then scanned targets of varying height through the small, dorso–frontal receptive fields (Fig. 3*A*) to confirm that each neuron was sharply size tuned with a peak response to targets subtending 3° to 6°, with no response to larger bars to looming or to widefield stimuli (22, 24).

Unless otherwise mentioned, targets were black and round with a diameter of 15 pixels, moving at a velocity of 900 pixels/s for 0.48 s. When converted to angular values and taking the small frontal receptive fields of TSDNs into account, this corresponds to an average diameter of 3° and a velocity of 130°/s (22). Unless otherwise stated, each target traveled in each neuron's preferred horizontal direction (i.e., left or right) and across the center of its receptive field. Between repetitions, we varied the target elevation slightly, to minimize habituation (22). There was a minimum 4 s between stimulus presentations. Stimulus order was randomized.

Optic flow was generated as previously described (24). Briefly, the optic flow consisted of a simulated cube with 4-m sides, filled with 2-cm-diameter spheres at a density of 100/m^3, unless otherwise stated, with the hoverfly placed in the center. The motion of these randomly placed circa 6,400 spheres around the hoverfly was used to simulate self-generated optic flow. The circa 1,200 spheres anterior to the hoverfly were projected onto the screen, with their size indicating the distance from the hoverfly. Circles closer than 6 cm were not displayed. Six types of optic flow were simulated: three translations at 50 cm/s (sideslip, lift, and thrust) and three rotations at 50°/s (yaw, pitch, and roll). Unless otherwise stated, optic flow was displayed for 0.48 s prior to the target. Both target motion and optic flow disappeared simultaneously.

In most experiments, the optic flow covered the entire visual display. In some experiments, we limited the spatial extent of the optic flow into four spatial positions. TSDN receptive fields tend to be located slightly offset from the visual midline, with preferred direction of motion away from the midline (Fig. 3*A*). We defined the lateral parts of the display as either ipsilateral or contralateral based on the preferred direction of each TSDN.

Data Analysis and Statistics. We recorded from 39 TSDNs in 39 male hoverflies. We kept data from all TSDNs that showed a robust response to a target moving over a white background (Fig. 1 and Movies S1 and S2). We repeated this control throughout the recording and only kept data from neurons that responded consistently. We only kept data from experiments with a minimum nine repetitions. The data from repetitions within a neuron were averaged and shown as spike histograms (mean ± SEM) with 1-ms resolution, after smoothing with a 20-ms square-wave filter. For quantification across neurons, we calculated the mean spike rate for each neuron from the spike histogram for the duration of target motion, after excluding the first and last 40 ms of each 0.48 s target trajectory (dotted boxes, Fig. 1 *B* and *C*), unless otherwise indicated. We normalized the responses to each neuron's own mean response to a target moving over a white background. Percentage change was defined as $(\text{Response}_{\text{experimental condition}} - \text{Response}_{\text{stationary control}})/\text{Response}_{\text{stationary control}}$.

Data analysis was performed in Matlab and statistical analysis in Prism 7.0c for Mac OS X (GraphPad Software). Throughout the paper, *n* refers to the number of repetitions within one neuron and *N* to the number of neurons. The sample size, type of test (paired *t* tests or one-way ANOVAs, followed by Dunnett's post hoc test for multiple comparisons), and *P* value are indicated in each figure legend. All data have been deposited to DataDryad (https://doi.org/10.5061/dryad.rn8pk0p6z).

Data Availability. Prism files data have been deposited in DataDryad (https://doi.org/10.5061/dryad.rn8pk0p6z).

ACKNOWLEDGMENTS. We thank current and past laboratory members for constructive feedback and the Botanic Gardens of Adelaide for their ongoing support. Malin Thyselius provided the hoverfly pictogram in Fig. 2 and *SI Appendix*, Fig. S4. Our research was funded by the US Air Force Office of Scientific Research (FA9550-19-1-0294), the Australian Research Council (DP170100008, DP180100144 and FT180100289), and the Flinders Foundation.

1. P. T. Gonzalez-Bellido, S. T. Fabian, K. Nordström, Target detection in insects: Optical, neural and behavioral optimizations. *Curr. Opin. Neurobiol.* **41**, 122–128 (2016).
2. W. Wellington, S. Fitzpatrick, Territoriality in the drone fly, *Eristalis tenax* (Diptera, Syrphidae). *Can. Entomol.* **113**, 695–704 (1981).
3. J. Zeil, Sexual dimorphism in the visual system of flies: The free flight behavior of male Bibionidae (Diptera). *J. Comp. Physiol. A Neuroethol. Sens. Neural Behav. Physiol.* **150**, 395–412 (1983).
4. S. T. Fabian, M. E. Sumner, T. J. Wardill, S. Rossoni, P. T. Gonzalez-Bellido, Interception by two predatory fly species is explained by a proportional navigation feedback controller. *J. R. Soc. Interface* **15**, 20180466 (2018).
5. R. Schröder, C. N. Linkem, J. A. Rivera, M. A. Butler, Should I stay or should I go? Perching damselfly use simple colour and size cues to trigger flight. *Anim. Behav.* **145**, 29–37 (2018).
6. C. T. O'Rourke, T. Pitlik, M. Hoover, E. Fernández-Juricic, Hawk eyes II: Diurnal raptors differ in head movement strategies when scanning from perches. *PLoS One* **5**, e12169 (2010).
7. S. M. Fitzpatrick, W. G. Wellington, Contrasts in the territorial behavior of three species of hover flies (Diptera: Syrphidae). *Can. Entomol.* **115**, 559–566 (1983).
8. E. L. Corvidae, R. O. Bierregaard, S. E. Peters, Comparison of wing morphology in three birds of prey: Correlations with differences in flight behavior. *J. Morphol.* **267**, 612–622 (2006).
9. J. J. Koenderink, Optic flow. *Vision Res.* **26**, 161–179 (1986).
10. W. Reichardt, M. Egelhaaf, A. Guo, Processing of figure and background motion in the visual system of the fly. *Biol. Cybern.* **61**, 327–345 (1989).
11. S. Cabrera, J. C. Theobald, Flying fruit flies correct for visual sideslip depending on relative speed of forward optic flow. *Front. Behav. Neurosci.* **7**, 76 (2013).
12. W. Reichardt, T. Poggio, Visual control of orientation behaviour in the fly. Part I. A quantitative analysis. *Q. Rev. Biophys.* **9**, 311–375, 428–438 (1976).
13. J. L. Fox, M. A. Frye, Figure-ground discrimination behavior in *Drosophila*. II. Visual influences on head movement behavior. *J. Exp. Biol.* **217**, 570–579 (2014).
14. A. J. Kim, J. K. Fitzgerald, G. Maimon, Cellular evidence for efference copy in *Drosophila* visuomotor processing. *Nat. Neurosci.* **18**, 1247–1255 (2015).
15. M. Egelhaaf, R. Kern, J. P. Lindemann, Motion as a source of environmental information: A fresh view on biological motion computation by insect brains. *Front. Neural Circuits* **8**, 127 (2014).
16. B. R. Geurten, R. Kern, E. Braun, M. Egelhaaf, A syntax of hoverfly flight prototypes. *J. Exp. Biol.* **213**, 2461–2475 (2010).
17. N. Boeddeker, L. Dittmar, W. Stürzl, M. Egelhaaf, The fine structure of honeybee head and body yaw movements in a homing task. *Proc. Biol. Sci.* **277**, 1899–1906 (2010).
18. J. M. Mongeau, M. A. Frye, Drosophila spatiotemporally integrates visual signals to control saccades. *Curr. Biol.* **27**, 2901–2914.e2 (2017).
19. T. S. Collett, Angular tracking and the optomotor response. An analysis of visual reflex interaction in a hoverfly. *J. Comp. Physiol. A Neuroethol. Sens. Neural Behav. Physiol.* **140**, 145–158 (1980).
20. D. O'Carroll, Feature-detecting neurons in dragonflies. *Nature* **362**, 541–543 (1993).
21. K. Nordström, P. D. Barnett, D. C. O'Carroll, Insect detection of small targets moving in visual clutter. *PLoS Biol.* **4**, e54 (2006).
22. S. Nicholas, J. Supple, R. Leibbrandt, P. T. Gonzalez-Bellido, K. Nordström, Integration of small- and wide-field visual features in Target-Selective Descending Neurons of both predatory and non-predatory dipterans. *J. Neurosci.* **38**, 10725–10733 (2018).

23. M. A. Frye, R. M. Olberg, Visual receptive field properties of feature detecting neurons in the dragonfly. *J. Comp. Physiol. A Neuroethol. Sens. Neural Behav. Physiol.* **177**, 569–576 (1995).
24. S. Nicholas, R. Leibbrandt, K. Nordström, Visual motion sensitivity in descending neurons in the hoverfly. *J. Comp. Physiol. A Neuroethol. Sens. Neural Behav. Physiol.* **206**, 149–163 (2020).
25. P. T. Gonzalez-Bellido, H. Peng, J. Yang, A. P. Georgopoulos, R. M. Olberg, Eight pairs of descending visual neurons in the dragonfly give wing motor centers accurate population vector of prey direction. *Proc. Natl. Acad. Sci. U.S.A.* **110**, 696–701 (2013).
26. P. D. Barnett, K. Nordström, D. C. O'carroll, Retinotopic organization of small-field-target-detecting neurons in the insect visual system. *Curr. Biol.* **17**, 569–578 (2007).
27. A. D. Straw, E. J. Warrant, D. C. O'Carroll, A "bright zone" in male hoverfly (*Eristalis tenax*) eyes and associated faster motion detection and increased contrast sensitivity. *J. Exp. Biol.* **209**, 4339–4354 (2006).
28. G. A. Horridge, The separation of visual axes in apposition compound eyes. *Philos. Trans. R. Soc. Lond. B Biol. Sci.* **285**, 1–59 (1978).
29. R. M. Olberg, Identified target-selective visual interneurons descending from the dragonfly brain. *J. Comp. Physiol. A Neuroethol. Sens. Neural Behav. Physiol.* **159**, 827–840 (1986).
30. C. T. Hsu, V. Bhandawat, Organization of descending neurons in *Drosophila melanogaster*. *Sci. Rep.* **6**, 20259 (2016).
31. R. M. Olberg, *Visual and Multimodal Interneurons in Dragonflies* (University of Washington, Seattle, 1978).
32. O. Dyakova, M. M. Müller, M. Egelhaaf, K. Nordström, Image statistics of the environment surrounding freely behaving hoverflies. *J. Comp. Physiol. A Neuroethol. Sens. Neural Behav. Physiol.* **205**, 373–385 (2019).
33. C. Städele, M. F. Keleş, J. M. Mongeau, M. A. Frye, Non-canonical receptive field properties and neuromodulation of Feature-Detecting neurons in flies. *Curr. Biol.* **30**, 2508–2519.e6 (2020).
34. M. O. Franz, H. G. Krapp, Wide-field, motion-sensitive neurons and matched filters for optic flow fields. *Biol. Cybern.* **83**, 185–197 (2000).
35. O. Dyakova, Y.-J. Lee, K. D. Longden, V. G. Kiselev, K. Nordström, A higher order visual neuron tuned to the spatial amplitude spectra of natural scenes. *Nat. Commun.* **6**, 8522 (2015).
36. K. Nordström, D. C. O'Carroll, Feature detection and the hypercomplex property in insects. *Trends Neurosci.* **32**, 383–391 (2009).
37. M. F. Keleş, B. J. Hardcastle, C. Städele, Q. Xiao, M. A. Frye, Inhibitory interactions and columnar inputs to an object motion detector in *Drosophila*. *Cell Rep.* **30**, 2115–2124.e5 (2020).
38. M. F. Keleş, M. A. Frye, Object-detecting neurons in *Drosophila*. *Curr. Biol.* **27**, 680–687 (2017).
39. R. Tanaka, D. A. Clark, Object-displacement-sensitive visual neurons drive freezing in *Drosophila*. *Curr. Biol.* **30**, 2532–2550.e8 (2020).
40. M. Egelhaaf, On the neuronal basis of figure-ground discrimination by relative motion in the visual system of the fly. II. Figure-detection cells, a new class of visual interneurones. *Biol. Cybern.* **52**, 195–209 (1985).
41. A. K. Warzecha, M. Egelhaaf, A. Borst, Neural circuit tuning fly visual interneurons to motion of small objects. I. Dissection of the circuit by pharmacological and photoinactivation techniques. *J. Neurophysiol.* **69**, 329–339 (1993).
42. W. Reichardt, T. Poggio, Figure-ground discrimination by relative movement in the visual-system of the fly. Part I: Experimental results. *Biol. Cybern.* **35**, 81–100 (1979).
43. T. Collett, Visual neurones in the anterior optic tract of the privet hawk moth. *J. Comp. Physiol.* **78**, 396–433 (1972).
44. S. D. Wiederman, P. A. Shoemaker, D. C. O'Carroll, A model for the detection of moving targets in visual clutter inspired by insect physiology. *PLoS One* **3**, e2784 (2008).
45. M. Egelhaaf, On the neuronal basis of figure-ground discrimination by relative motion in the visual system of the fly. III. Possible input circuitries and behavioral significance of the FD-cells. *Biol. Cybern.* **52**, 267–280 (1985).
46. S. D. Wiederman, P. A. Shoemaker, D. C. O'Carroll, Correlation between OFF and ON channels underlies dark target selectivity in an insect visual system. *J. Neurosci.* **33**, 13225–13232 (2013).
47. S. D. Wiederman, D. C. O'Carroll, Discrimination of features in natural scenes by a dragonfly neuron. *J. Neurosci.* **31**, 7141–7144 (2011).
48. S. Nicholas, K. Nordström, Persistent firing and adaptation in optic flow sensitive descending neurons. *Curr. Biol.* **30**, 2739–2748.e2 (2020).
49. T. S. Collett, M. F. Land, How hoverflies compute interception courses. *J. Comp. Physiol. A Neuroethol. Sens. Neural Behav. Physiol.* **125**, 191–204 (1978).
50. J. L. Fox, J. W. Aptekar, N. M. Zolotova, P. A. Shoemaker, M. A. Frye, Figure-ground discrimination behavior in *Drosophila*. I. Spatial organization of wing-steering responses. *J. Exp. Biol.* **217**, 558–569 (2014).
51. B. Cellini, J. M. Mongeau, Active vision shapes and coordinates flight motor responses in flies. *Proc. Natl. Acad. Sci. U.S.A.* **117**, 23085–23095 (2020).
52. L. Varennes, H. G. Krapp, S. Viollet, Two pursuit strategies for a single sensorimotor control task in blowfly. *Sci. Rep.* **10**, 20762 (2020).
53. S. Nicholas, M. Thyselius, M. Holden, K. Nordström, Rearing and long-term maintenance of *Eristalis tenax* hoverflies for research studies. *J. Vis. Exp.*, 10.3791/57711 (2018).
54. D. H. Brainard, The Psychophysics toolbox. *Spat. Vis.* **10**, 433–436 (1997).
55. D. G. Pelli, The VideoToolbox software for visual psychophysics: Transforming numbers into movies. *Spat. Vis.* **10**, 437–442 (1997).